Supplemental Table S1. PCR Primers

Genetic manipulations	
rPRL transgene	5' CCTCCTCATTCTCTGCTCTTC 3' 5' CCAATCACCCTTGCTCTAAACCC 3'
Apc^{Min} germline mutation	5' TGAGAAAGACAGAAGTTA 3' 5' TTCCACTTTGGCATAAGGC 3' Internal control, 5'GCCATCCCTTCACGTTAG
Apc hotspot region (aa 1512-1579), sequencing tags in bold	5' **GTT TTC CCA GTC ACG AC**C CAA GCA GAA GCA AAA CCC C 3' 5' **CAG GAA ACA GCT ATG A**CC CTC GCT GAG CAT CAT CTG T 3'
qRT-PCR	
18S	F, 5' CGC CGC TAG AGG TGA ATT TCT 3' R, 5' CGA ACC TCC GAC TTT CGT TCT 3'
Axin2	F, 5' CCA GGC TGG AGA AAC TGA AAC T 3' R, 5' CCT GCT CAG ACC CCT CCT TT 3'
Ccnd1	F, 5' CAT CAA GTG TGA CCC GGA CTG 3' R, 5' CCT CCT CCT CAG TGG CCT TG 3'
Ccne1	F, 5' GCC AAG ATT GAC AAG ACT GTG AAA 3' R, 5' GGT CCA CGC ATG CTG AAT TA 3'
Cdkn2c	F, 5' CAA CGC CCC GAA CTC TTT C 3' R, 5' AGC AGA AGA GCT GCT ACG TGA A 3'
Hes1	F, 5' TAC CCC AGC CAG TGT CAA CA 3' R, 5' CCT TCG CCT CTT CTC CAT GA 3'
Hey1	F, 5' GGT ACC CAG TGC CTT TGA GA 3' R, 5' GGC GTG CGC GTC AAA ATA A 3'
Nrarp	F, 5' CCA GCG TTG TGA AGG CTG TT 3' R, 5' GCA GCC CTT CCA CTC ATT CA 3'
Notch1	F, 5' ACA ACA ACG AGT GTG AGT CC 3' R, 5' ACA CGT GGC TCC TGT ATA TG 3'
Notch2	F, 5' TAC CTA CCA CAA CGG CAC AG 3' R, 5' TCT CAC AGG GGT CTC GAT GT 3'

Notch3	F, 5’ AGA TCA ATG AGT GTG CAT CC 3’ R, 5’ GCA GAC TCC ATG ACT ACA GG 3’
Notch4	F, 5’ AAT GGG GGT ACC TGT GTG AA 3’ R, 5’ GTA TAG CCA GGG CTG CAG AG 3’
Sox2	F, 5’ CCA CCA ATC CCA TCC AAA TT 3’ R, 5’ CAA AAA GAA GTC CCA AGA TCT CTC A 3’
Sox9	F, 5’ CGA GCA CTC TGG GCA ATC TC 3’ R, 5’ CCT CTC GCT TCA GAT CAA CTT TG 3’
Tcf4	F, 5’ CCT CGT CAT CTC CCA ATT ATG AA 3’ R, 5’ GTC TTT CCA AAC GGT CTT CGA T 3’

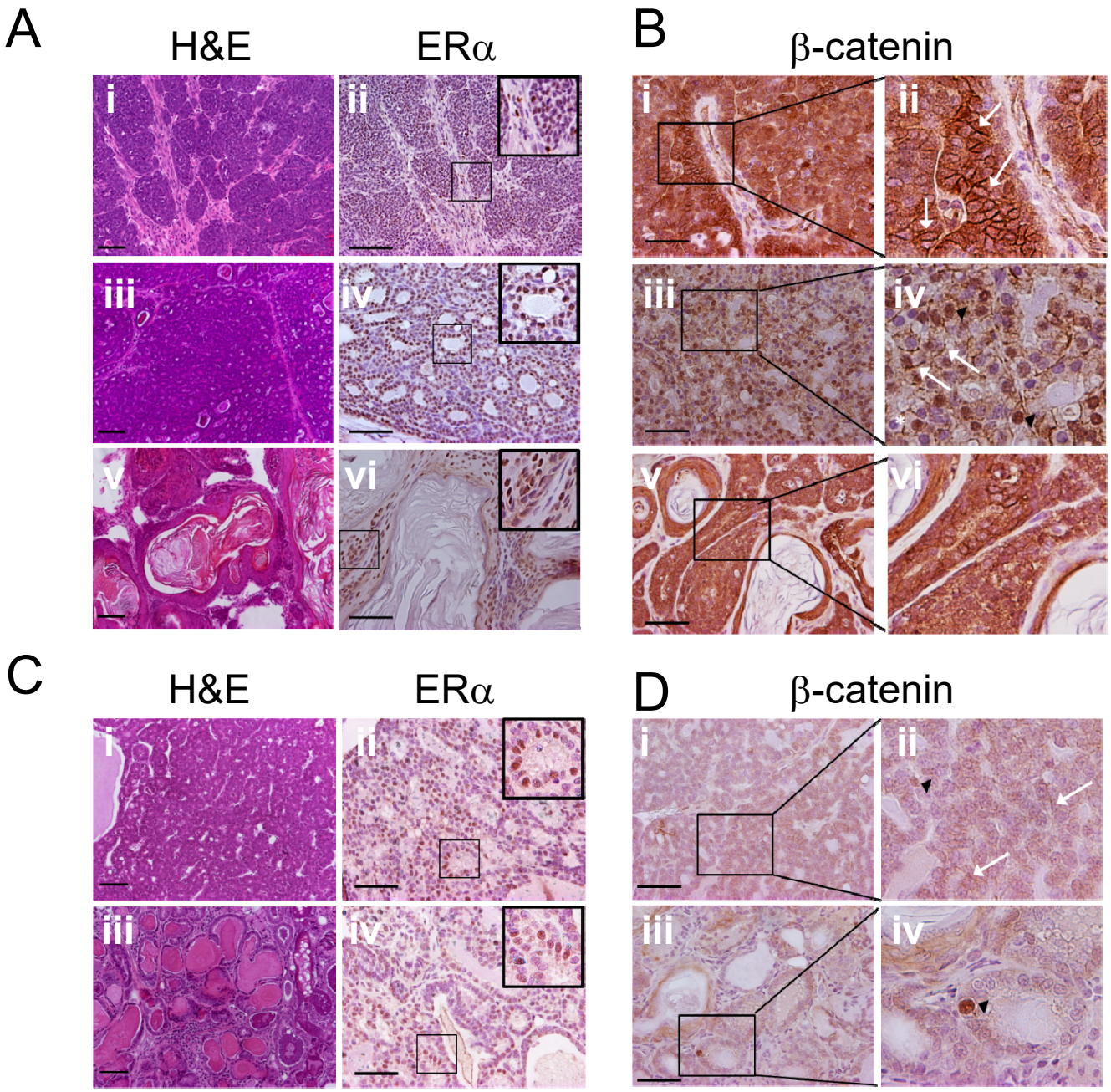

Suppl. Fig. S1. **Tumors from *Apc*$^{Min/+}$ (A,B) and NRL-PRL (C,D) females.** (A) *Apc*$^{Min/+}$ tumors. Left, hematoxylin and eosin (H&E) stained representative histotypes (i, ii, glandular; iii, iv, microacinar; v, vi, adenosquamous). Right, ERα expression by immunohistochemistry; insets as shown. (B) Tumors from *Apc*$^{Min/+}$ females exhibited heterogeneous cellular localization of β-catenin; insets as shown. (i, ii, glandular; iii, iv, microacinar; v, vi, adenosquamous). (C) Tumors from NRL-PRL females. Left, H&E stained histotypes (i, ii, glandular; iii, iv, papillary). Right, ERα expression by immunohistochemistry; insets as shown. (D) Tumors that developed NRL-PRL females exhibited lower β-catenin expression compared to tumors from *Apc*$^{Min/+}$ and NRL-PRL/*Apc*$^{Min/+}$ females; insets as shown. (i, ii, glandular; iii, iv, papillary). White arrows indicate membrane β-catenin, black arrowheads indicate nuclear β-catenin, and white asterisk shows cell with negligible detectable β-catenin. Scale bars, 100 µm. Original magnifications, H&E, x100; β-catenin, ERα, x200.

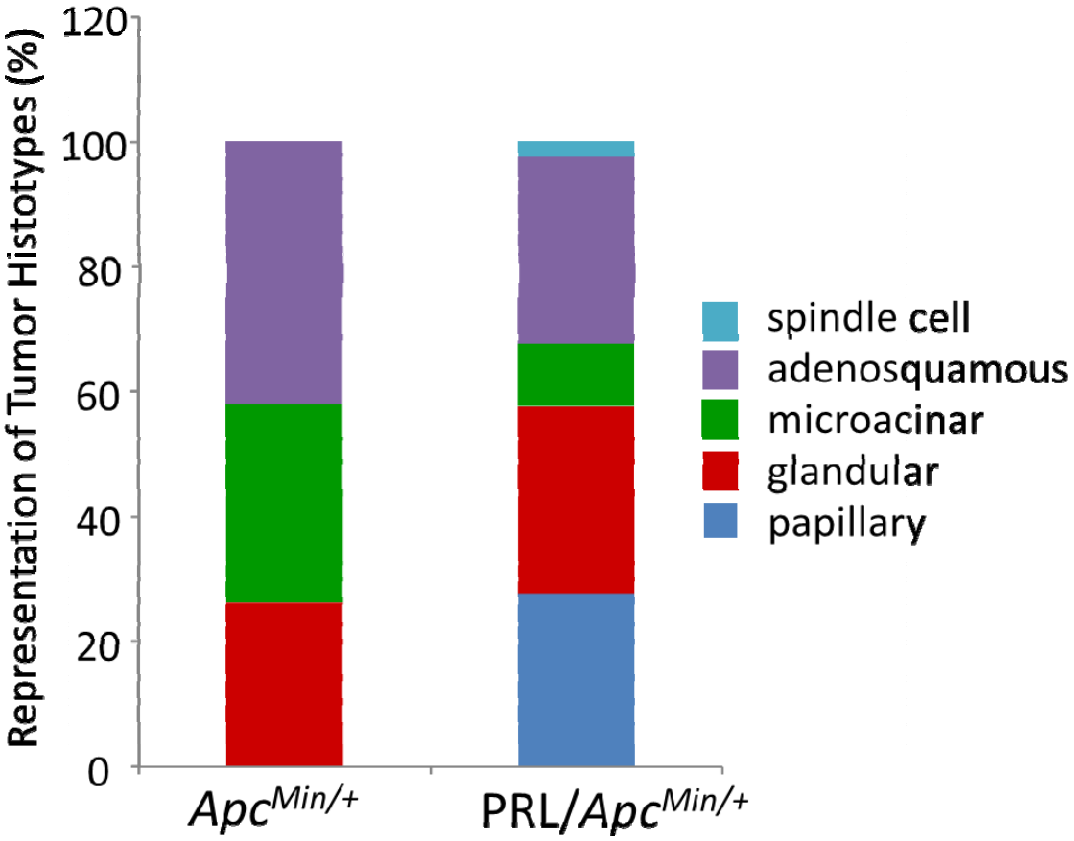

Suppl. Fig. S2. Tumors that develop in *Apc*$^{Min/+}$ and NRL-PRL/*Apc*$^{Min/+}$ females exhibit similar spectra of histotypes, except that papillary carcinomas develop only in the presence of PRL. N= 19 tumors in *Apc*$^{Min/+}$ females; N=40 tumors in NRL-PRL/*Apc*$^{Min/+}$ females. Tumors in NRL-PRL females are not shown because of the low number of tumors (2 x papillary, 1 glandular. N=3).

A

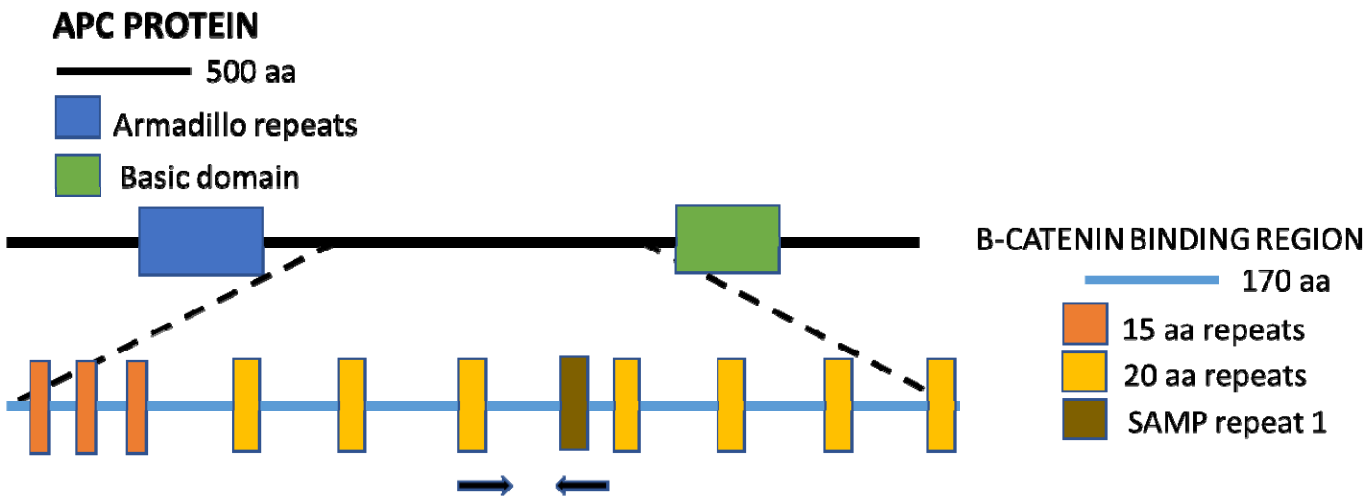

B

Mutation	*Apc*$^{min/+}$	PRL/*Apc*$^{min/+}$	Histotype
None		4	adenosquamous, papillary, 2 x glandular
AA1512 (G/T)AG		1	adenosquamous
AA1516 (C/T)AG		2	2 x adenosquamous
AA1521 T(T/A)A		1	papillary
AA1521 T(T/G)A		3	adenosquamous, 2 x glandular
AA1528 (C/T)AG	1		adenosquamous
AA1529 (G/T)AA	1		adenosquamous
AA1531 **G**GAC		1	glandular
AA1539 (G/T)AA	1	1	2 x glandular
AA1540 (C/T)AG	1	2	adenosquamous, 2 x papillary
AA1548 (C/T)AG		1	glandular
AA1561 T(T/A)A	1		adenosquamous
AA1562 T(T/G)A	1		microacinar
AA1568 ~~G~~AT	1	1	glandular, adenoquamous
AA1569 ~~G~~AT	1		adenosquamous
AA1576 TG(T/A)	1		glandular
TOTAL	9/9 (100.0%)	13/17 (76.5%)	
#/ total #(percentage)			

~~N~~ strikethrough: deletion

NN bold: insertion

Suppl. Fig. S3. Tumors in PRL/ *Apc*$^{Min/+}$ and *Apc*$^{Min/+}$ females acquire a somatic mutation in the second *Apc* allele. (A) Diagram of the APC protein. Expanded area, β-catenin binding region. Arrows indicate the region where somatic mutations cluster in mammary tumors in mutant *Apc* models (Kuraguchi et al., 2009; Keller et al., 2016). This region was sequenced in a subset of tumors in this study. aa, amino acids. (B) Somatic mutations detected in tumors in this region of the *Apc* gene in *Apc*$^{Min/+}$ and NRL-PRL-*Apc*$^{Min/+}$ ENU-treated females.

A

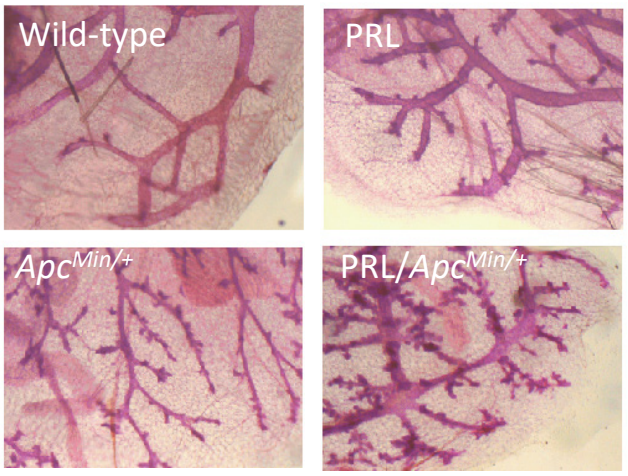

B

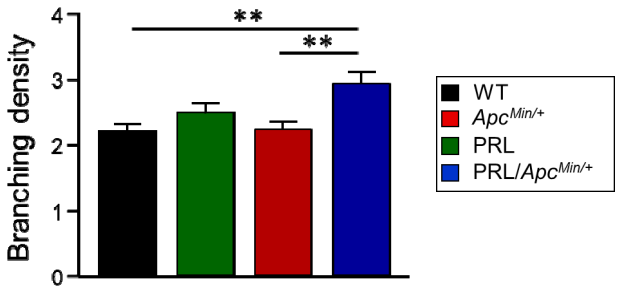

C

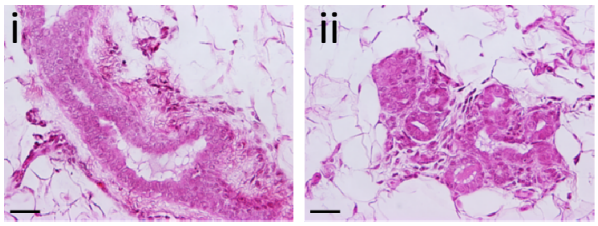

D **Incidence of microscopic mammary abnormalities in 120 d.o. ENU-treated females[a]**

	WT	*Apc*$^{Min/+}$	NRL-PRL	NRL-PRL/*Apc*$^{Min/+}$
Focal irregular ductal epithelium[b]	(0/7)	(5/7)	(2/6)	(5/6)
Focal epithelial hyperplasias				
Small[c]	(2/7)	(7/7)	(6/6)	(6/6)
Large[d]	(0/7)	(7/7)	(0/6)	(6/6)
Squamous changes[e]	(0/7)	(6/7)	(0/6)	(5/6)

[a]Number of mice exhibiting lesions/ total number of mice examined in H&E stained sections.
[b]Illustrated in Fig. S4CI
[c]Small epithelial hyperplasias were defined as structures with 5-20 lumens, each surrounded by cuboidal epithelial cells (illustrated in Fig. S4CII).
[d]Large epithelial hyperplasias were defined as structures with more than 20 lumens, each surrounded by cuboidal epithelial cells (illustrated in Fig. 4A)
[e]Illustrated in Fig. 4A.

Suppl. Fig. S4. PRL influences epithelial structures in 120 d.o. ENU-treated females, but in the absence of *Apc*$^{Min/+}$, few mammary abnormalities are observed. (A) PRL cooperates with *Apc*$^{Min/+}$ to increase ductal branching. Representative mammary whole mounts, stained with carmine alum. (B) Quantitation of ductal branching (mean ± S.E.M. **, $p<0.01$; N=4-7). (C) Image of (i) irregular ductal epithelium; and (ii) small epithelial hyperplasia (Hematoxylin/eosin stain). Scale bars, 100 µm. Original magnifications, x200. (D) Incidence of microscopic mammary abnormalities.

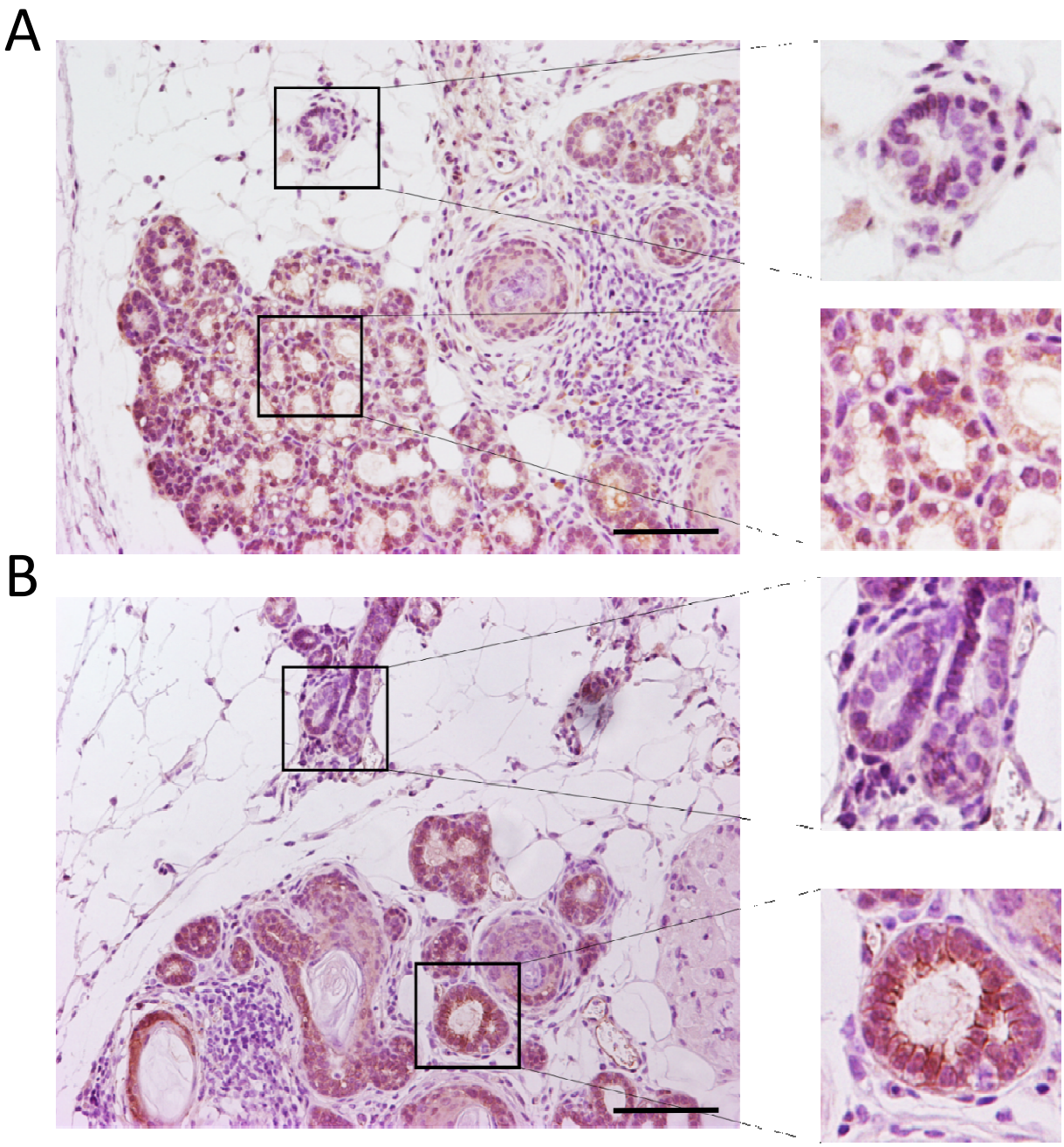

Suppl. Fig. S5. Ductal luminal epithelium does not accumulate β-catenin in either *Apc*$^{Min/+}$ or NRL-PRL/*Apc*$^{Min/+}$ 120 d.o. ENU-treated females. (A) Large epithelial hyperplasias in mammary glands of ENU-treated *Apc*$^{Min/+}$ females exhibited abundant nuclear β-catenin, which was not evident in ductal structures. (B) Epithelial hyperplasias in mammary glands of ENU-treated NRL-PRL *Apc*$^{Min/+}$ females exhibited abundant β-catenin at the plasma membrane, which was not evident in ductal structures. (A,B) Upper right insets, ductal structures; lower insets, epithelial hyperplasias. Scale bar, 500 mm. Original magnifications, x100.

A *Apc*$^{Min/+}$ B NRL-PRL/*Apc*$^{Min/+}$

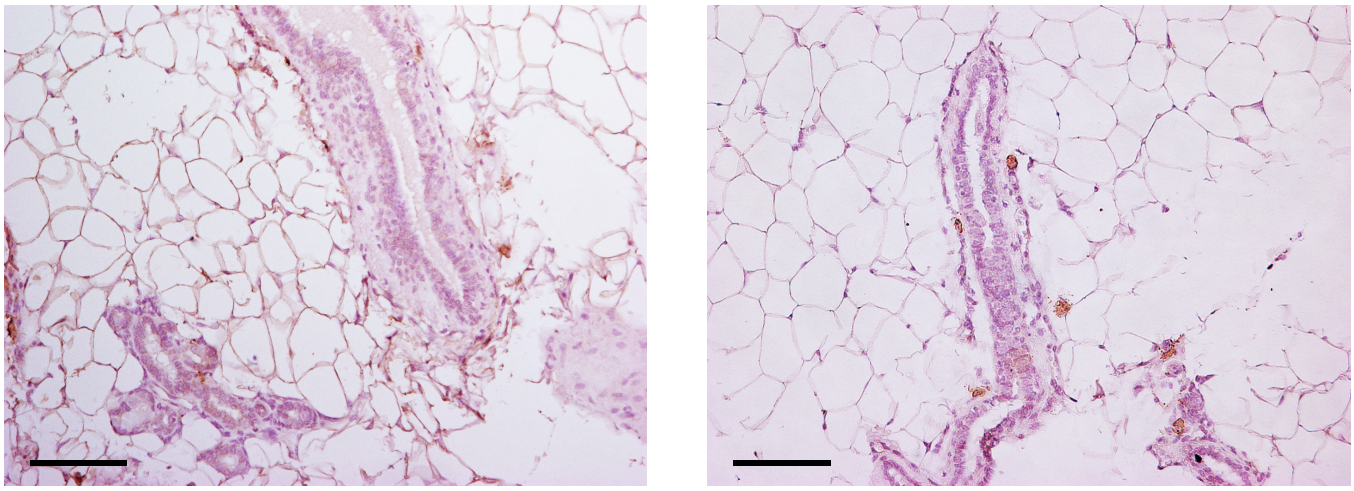

Suppl. Fig. S6. Ductal luminal epithelium expresses little NOTCH1 in either *Apc*$^{Min/+}$ or NRL-PRL/*Apc*$^{Min/+}$ 120 d.o. ENU-treated females. (A) Mammary gland from *Apc*$^{Min/+}$ female. (B) Mammary gland from NRL-PRL/*Apc*$^{Min/+}$ female. Scale bar, 500 mm. Original magnifications, x100.